2 Thickness mode resonators

2.1 WAVE PROPAGATION IN PIEZOELECTRIC MATERIALS

The subject of the propagation of elastic waves in solid materials has a long history, although the extension of the analysis to give a complete treatment in the piezoelectric case has only been made relatively recently. The book *Linear Piezoelectric Plate Vibrations* by Tiersten (1969), and the review article *Doubly Rotated Thickness Mode Plate Vibrators* by Ballato (1977) should be consulted for references to the earlier work.

The field equations and constitutive relations for a linear piezoelectric material are (Appendix 4)

$$t_{kl,l} = \rho \ddot{u}_k \tag{2.1}$$

$$D_{k,k} = 0 \tag{2.2}$$

$$E_k = -\phi_{,k} \tag{2.3}$$

$$t_{kl} = c_{klmn} S_{mn} - e_{mkl} E_m \tag{2.4}$$

$$D_k = e_{klm} S_{lm} + \epsilon_{kl} E_l \tag{2.5}$$

where ρ is the mass density, u_k the particle displacement, E_k, D_k and ϕ are the electric field, displacement and potential respectively, t_{kl} and S_{kl} are the elastic stress and strain, and c_{klmn}, e_{klm} and ϵ_{kl} are the elastic, piezoelectric and dielectric constants. For any function f, differentiation with respect to the position coordinate x_k is denoted by $f_{,k}$, whereas the partial derivative with respect to the time is written $\dot{f}$. The strain S_{kl} is defined in terms of the displacements u_k by

$$S_{kl} = (u_{k,l} + u_{l,k})/2 \tag{2.6}$$

Using Eqns (2.3) to (2.6), the field equations (2.1) and (2.2) can be expressed in terms of the displacements u_k and the potential ϕ by

$$c_{klmn} u_{m,nl} + e_{mkl} \phi_{,ml} = \rho \ddot{u}_k \tag{2.7}$$

$$e_{klm} u_{l,mk} - \epsilon_{kl} \phi_{,lk} = 0 \tag{2.8}$$

For solutions to Eqns (2.7) and (2.8) in the form of plane waves propa-

gating along an arbitrary direction specified by a unit vector n_k, the field variables reduce to functions of the distance $x = n_k x_k$ measured along n_k. Then for any field f, the spatial derivatives $f_{,k}$ are given by $n_k f_{,x}$, where $f_{,x}$ denotes the derivative with respect to x. Consequently, Eqns (2.7) and (2.8) become

$$L_{km} u_{m,xx} + e_k \phi_{,xx} = \rho \ddot{u}_k \tag{2.9}$$

$$e_m u_{m,xx} - \epsilon \phi_{,xx} = 0 \tag{2.10}$$

with the definitions

$$L_{km} = c_{klmn} n_l n_n \tag{2.11}$$

$$e_l = e_{klm} n_k n_m \tag{2.12}$$

$$\epsilon = \epsilon_{kl} n_k n_l \tag{2.13}$$

Equation (2.10) can immediately be integrated to give the potential in terms of the displacements

$$\phi = e_k u_k / \epsilon + Cx + D \tag{2.14}$$

where C and D are arbitrary functions of the time t but independent of x. Also, Eqn (2.10) can be used to eliminate ϕ from Eqn (2.9), leading to

$$\bar{L}_{km} u_{m,xx} = \rho \ddot{u}_k \tag{2.15}$$

$$\bar{L}_{km} = L_{km} + e_k e_m / \epsilon \tag{2.16}$$

The surface tractions across a surface normal to n_k are given by $t_k = t_{kl} n_l$, and the normal component of the electric displacement is $D_k n_k$. From the constitutive relations (2.4) and (2.5)

$$t_k = L_{km} u_{m,x} + e_k \phi_{,x}$$

$$D_k n_k = e_l u_{l,x} - \epsilon \phi_{,x}$$

Substituting for ϕ from Eqn (2.14) gives

$$t_k = \bar{L}_{km} u_{m,x} + e_k C \tag{2.17}$$

$$D_k n_k = -\epsilon C \tag{2.18}$$

Because of the symmetry of the elastic constants expressed by the relation $c_{klmn} = c_{mnkl}$, the L_{km}, and therefore also the $\bar{L}_{km}$, are the components of symmetric second rank tensors. As shown in Appendix 4, the form $L_{km} x_k x_m$ is positive definite, and since

$$\bar{L}_{km} x_k x_m = L_{km} x_k x_m + (e_k x_k)^2 / \epsilon$$

it follows that $\bar{L}_{km} x_k x_m$ is also positive definite. Hence (Section A2.6) a coordinate system can be found in which $\bar{L}_{km} = \delta_{km} c_m$ (no sum over m) and in which all the eigenvalues c_m are positive. In this special coordinate system, the wave equation, Eqn (2.15), separates into three uncoupled equations for the three displacement components

$$c_k u_{k,xx} = \rho \ddot{u}_k \qquad \text{(no sum on } k\text{)} \tag{2.19}$$

For each k, $k = 1, 2$ and 3, Eqn (2.19) is an elementary one-dimensional wave equation, representing waves propagating along x with a phase velocity $V_k = (c_k/\rho)^{1/2}$ and c_k representing an effective elastic constant. Clearly, by the choice of coordinate system, the particle displacement for the wave with velocity V_k is along the x_k axis, so that the particle displacements for the three waves are mutually orthogonal.

This is strictly true only when the phase velocities V_k are all unequal. In the degenerate case when two of the velocities have equal magnitudes, then clearly any linear combination of the corresponding displacements will also propagate with the same velocity; nevertheless, it is always possible to resolve any such waves into two components with mutually perpendicular displacements.

Physically, the preceding analysis means that for an arbitrary direction in an elastic or piezoelectric material, there will in general be three possible types of plane wave, distinguished by different phase velocities and mutually perpendicular particle displacements. In the special case of an isotropic material, and also in certain directions of high symmetry in crystalline materials, the coordinate system that diagonalizes Γ_{km} is such that the propagation direction lies along one of the axes. The three wave types can then be classified as longitudinal and transverse, the longitudinal wave being characterized by the particle displacement lying along the direction of propagation, whereas the two transverse waves have the particle displacement at right angles to the propagation direction. Generally, however, this will not be the case, and the longitudinal/transverse classification will at best serve as an approximate indication of the wave character.

2.2 BOUNDARY CONDITIONS FOR THICKNESS MODES

Thickness mode resonators are typically cut in the form of thin, flat plates whose lateral dimensions are much greater than the thickness. In a first approximation, the analysis of such resonators is based on the physical idea of a system of standing waves set up in the resonator by plane waves propagating along the thickness and being reflected at the major surfaces of the plate. The lateral dimensions are assumed to be effectively infinite. Of course, this is an oversimplification of the real problem, and the effect of finite lateral dimensions (considered in Chapter 3) cannot be neglected in practice. Nevertheless, the pure thickness mode approximation provides a great deal of insight and understanding, particularly in the context of the properties of oblique crystal cuts.

As shown in the previous section, for each propagation direction three types of plane wave exist. In a resonator therefore it is to be anticipated that

there will be three distinct standing wave systems, which may or may not be coupled by the boundary conditions at the surfaces of the plate. Consider a resonator with major surfaces at $x = \pm h$ coated with massless, conducting electrodes that are connected to a voltage source of emf E. Then appropriate electrical boundary conditions are that the potential $\phi = \pm E/2$ at $x = \pm h$. Since the electrodes are assumed massless, the mechanical boundary conditions are simply that the surface tractions $t_k = t_{kl}n_l$ vanish at $x = \pm h$. Using Eqns (2.14) and (2.17) these conditions are

$$\phi(h) = e_k u_k(h)/\epsilon + Ch + D = E/2 \tag{2.20}$$

$$\phi(-h) = e_k u_k(-h)/\epsilon - Ch + D = -E/2 \tag{2.21}$$

$$t_k(h) = \Gamma_{km} u_{m,x}(h) + e_k C = 0 \tag{2.22}$$

$$t_k(-h) = \Gamma_{km} u_{m,x}(-h) + e_k C = 0 \tag{2.23}$$

Adding and subtracting Eqns (2.20) and (2.21) gives two equivalent equations

$$e_k[u_k(h) + u_k(-h)]/\epsilon + 2D = 0 \tag{2.24}$$

$$e_k[u_k(h) - u_k(-h)]/\epsilon + 2Ch = E \tag{2.25}$$

Similarly, adding and subtracting Eqns (2.22) and (2.23),

$$\Gamma_{km}[u_{m,x}(h) + u_{m,x}(-h)] + 2e_k C = 0 \tag{2.26}$$

$$\Gamma_{km}[u_{m,x}(h) - u_{m,x}(-h)] = 0 \tag{2.27}$$

Writing u_k as the sum of its symmetric and antisymmetric parts u_k^S and u_k^A and noting that the derivative of the symmetric part $u_{k,x}^S$ is antisymmetric in x and vice versa, Eqns (2.24) to (2.27) may be rewritten

$$e_k u_k^S(h)/\epsilon + D = 0 \tag{2.28}$$

$$e_k u_k^A(h)/\epsilon + Ch = E/2 \tag{2.29}$$

$$\Gamma_{km} u_{m,x}^A(h) + e_k C = 0 \tag{2.30}$$

$$\Gamma_{km} u_{m,x}^S(h) = 0 \tag{2.31}$$

with the definitions

$$u_k^S(x) = [u_k(x) + u_k(-x)]/2$$
$$u_k^A(x) = [u_k(x) - u_k(-x)]/2$$

Equations (2.28) to (2.31) reveal that the symmetric and antisymmetric parts of u_k are not coupled by the boundary conditions on the surface of the plate, and moreover that the symmetric part is not driven by the applied emf E, This is the fundamental reason why the symmetric even order overtones of thickness mode resonators cannot be electrically excited in normal circumstances (Section 1.4.1). In determining the resonance frequencies,

attention can thus be restricted to antisymmetric solutions of the wave equation (2.19).

2.3 RESONANCE FREQUENCIES AND ELECTROMECHANICAL COUPLING

The field equations and boundary conditions for antisymmetric functions u_k, when stated in the coordinate system for which Γ_{km} is diagonal, are

$$c_k u_{k,xx} = \rho \ddot{u}_k \qquad \text{(no sum on } k\text{)} \tag{2.19}$$

$$e_k u_k(h)/\epsilon + Ch = E/2 \tag{2.29a}$$

$$\Gamma_{km} u_{m,x}(h) + e_k C = 0 \tag{2.30a}$$

where by assumption $u_k = u_k^A$. Appropriate solutions to Eqn (2.19) are

$$u_k(x,t) = A_k \sin(\beta_k x)\exp(j\omega t) \qquad \text{(no sum on } k\text{)} \tag{2.32}$$

where the wavenumbers β_k are given by

$$c_k \beta_k^2 = \rho\omega^2 \qquad \text{(no sum on } k\text{)} \tag{2.33}$$

Writing C and E in the form $C_0\exp(j\omega t)$ and $E_0\exp(j\omega t)$, and cancelling the common factor $\exp(j\omega t)$, the boundary conditions become

$$\sum_k \left\{ e_k A_k \sin(X_k)/\epsilon \right\} + C_0 h = E_0/2 \tag{2.34}$$

$$\sum_k \left\{ \Gamma_{km} A_m B_m \cos(X_m) \right\} + e_k C_0 = 0 \tag{2.35}$$

where X_k has been written for $(\beta_k h)$. Since Γ_{km} is diagonal, Eqn (2.35) may be simplified to

$$c_k X_k A_k \cos(X_k) + e_k C_0 h = 0 \tag{2.36}$$

with there being no sum on k. Solving for the A_k gives

$$A_k = -e_k C_0 h/[c_k X_k \cos(X_k)] \tag{2.37}$$

and substituting in Eqn (2.34) gives a solution for C_0 in terms of the driving voltage E_0:

$$C_0 = (E_0/2h)/\left\{ 1 - \sum_m [k_m^2 \tan(X_m)/X_m] \right\} \tag{2.38}$$

where the *electromechanical coupling factor* for the mth mode, k_m, is defined by

$$k_m^2 = e_m^2/\epsilon c_m \qquad \text{(no } m \text{ sum)} \tag{2.39}$$

The current density in the resonator is given by $J = -j\omega D_k n_k$ and therefore from Eqn (2.18)

$$J = j\omega\epsilon C_0 = j\omega(\epsilon/2h)E_0/\left\{1 - \sum_m [k_m^2 \tan(X_m)/X_m]\right\} \tag{2.40}$$

Since $c_0 = (\epsilon/2h)$ is just the static capacitance of the plate per unit area, and E_0 is the applied voltage, the admittance y per unit area of the plate is given by

$$y = j\omega c_0/\left\{1 - \sum_m [k_m^2 \tan(X_m)/X_m]\right\} \tag{2.41}$$

The zeros and poles of the admittance correspond to the anti-resonance and resonance frequencies, respectively. The zeros coincide with the poles of the tangent functions in Eqn (2.40), and hence occur when $\cos(X_m) = 0$, or $X_m = M\pi/2$ where M is an odd integer. The corresponding frequencies are, from Eqn (2.33)

$$\begin{aligned} \omega &= (c_m/\rho)^{1/2}M\pi/2h \\ f &= (c_m/\rho)^{1/2}M/4h = MV_m/4h \end{aligned} \tag{2.42}$$

where V_m is the phase velocity of the mth mode. There are thus three harmonically related sequences of anti-resonance frequencies; if necessary, the notation $f_{mA}^{(M)}$ can be used to discriminate between them (Ballato, 1977).

The series resonance frequencies are determined by the zeros of the denominator of y, that is by the roots of the equation

$$\sum_m k_m^2 \tan(X_m)/X_m = 1 \tag{2.43}$$

Unlike the case of the anti-resonance frequencies, Eqn (2.43) does not generally allow the identification of separate sequences of roots each associated with a particular displacement mode. In the general case, for a given root of Eqn (2.43), all three modes will be excited. Obvious exceptions occur when one or two of the k_m vanish, since then the corresponding modes cannot be piezoelectrically excited. A very important case is that of the rotated Y-cut family, where only one k_m is non-zero, and only a single thickness shear mode excited. Even when two or three modes are excited, it may happen that conditions are such that one term in the sum in Eqn (2.43) dominates, so that as an approximation the other terms can be neglected. A detailed discussion will be found in Ballato (1977); the single mode case is briefly considered here in order to arrive at the important relationship between the coupling factor and the separation of the resonance and anti-resonance frequencies.

In the single mode case, Eqn (2.43) can be rewritten, dropping the suffices, as

$$\tan(X) = X/k^2 \tag{2.44}$$

Since for quartz, for all modes and all propagation directions, $k^2 \ll 1$, it

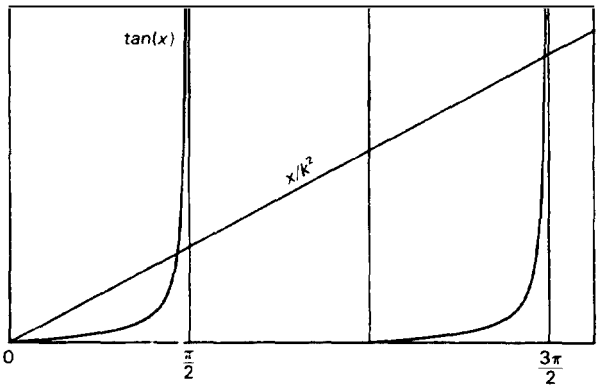

Fig. 2.1 Graphical solution of $\tan(X) = X/k^2$.

follows that the straight line X/k^2 has a much steeper slope than the tangent curve near the origin, as illustrated in Fig. 2.1. Therefore Eqn (2.44) will always have a root in the interval $[0, \pi/2]$, and an infinite sequence of roots thereafter, one in each of the intervals $[N\pi, (N + 1/2)\pi]$, for $N = 1,2,3. \ldots$ It is clear from the figure that as N increases, the roots tend to the poles of the tangent function, and that for fixed N, the separation between the root and the corresponding pole decreases as k decreases. Since as already pointed out, the poles of the tangent function correspond to the anti-resonance frequencies, the separation between resonance and anti-resonance frequencies diminishes with increasing N and decreasing k. Let $M = 2N + 1$ and let $X_R^{(M)}$ denote the root of Eqn (2.44) that lies in the interval $[N\pi, M\pi/2]$. Then if $X_A^{(M)} = M\pi/2$, and the fractional frequency difference $\delta_R^{(M)}$ is defined by

$$\delta_R^{(M)} = (X_A^{(M)} - X_R^{(M)})/X_A^{(M)} \tag{2.45}$$

$\delta_R^{(M)}$ is always $\ll 1$.

If for a general X, a corresponding δ is defined by

$$\delta = (X_A^{(M)} - X)/X_A^{(M)} \tag{2.46}$$

so that $X = X_A^{(M)}(1 - \delta)$, then $\tan(X) = \cot(\delta X_A^{(M)}$ and Eqn (2.44) can be rewritten as an equation in δ

$$k^2 = X_A^{(M)}(1 - \delta)\tan(\delta X_A^{(M)}) \tag{2.47}$$

For small δ the tangent can be replaced by its argument, and then to first order in δ, Eqn (2.47) has the solution

$$\delta_R^{(M)} = \delta = 4k^2/M^2\pi^2 \tag{2.48}$$

(Note: the fractional frequency difference defined above differs by a factor M from the *frequency displacement* defined by Ballato (Ballato, 1977))

2.4 EQUIVALENT CIRCUITS

Since the admittance y per unit area of the plate as defined by Eqn (2.41) has an infinite number of poles and zeros, no exact finite lumped parameter equivalent circuit exists. Equivalent circuits in the form of lengths of transmission lines have been proposed, but in the context of resonator theory and applications are unnecessarily cumbersome. For most practical purposes, it is entirely adequate to concentrate attention on the neighbourhood of a particular resonance frequency and employ a simple lumped element circuit valid only in that neighbourhood. Considering then the Mth order resonance of a plate in which only a single mode is excited (only one k_m non-zero), the admittance Y of an electrode patch of area A can be written in terms of the fractional frequency difference δ as

$$\begin{aligned} Y &= j\omega C_0/[1 - k^2\tan(X)/X] \\ &= j\omega C_0 X_A^{(M)}(1 - \delta)\tan(\delta X_A^{(M)})/[X_A^{(M)}(1 - \delta)\tan(\delta X_A^{(M)}) - k^2] \end{aligned}$$

where $C_0 = Ac_0 = A\epsilon/2h$. For small δ, this reduces to

$$Y = j\omega C_0 \delta/(\delta - \delta_R^{(M)}) \tag{2.49}$$

As anticipated, this expression has a single zero and a single pole, just as does the admittance, of the simple circuit of Fig. 2.2. The analysis of Section 6.2.1, shows that the fractional frequency difference between the pole and zero of Fig. 2.2 is determined by the capacitance ratio C_0/C_1. Therefore the equivalence is assured provided that

$$C_1/2C_0 = 4k^2/M^2\pi^2 \tag{2.50}$$

Since C_0 is known in terms of the electrode area, plate thickness and the effective dielectric constant ϵ, Eqn (2.50) determines C_1 in terms of the plate parameters. The inductance L_1 in Fig. 2.2 is of course determined by C_1 and the resonance frequency ω_r through $L_1 = 1/\omega_r^2 C_1$. Since the separation between resonance and anti-resonance is small, the simple expression Eqn (2.42) for the anti-resonance frequencies can be used in estimating L_1.

Summarizing, the parameters in the equivalent circuit are given by

$$\left.\begin{aligned} C_0 &= \epsilon A/2h \\ C_1 &= 8k^2 C_0/M^2\pi^2 = 4e^2 A/(chM^2\pi^2) \\ L_1 &= \rho h^3/(e^2 A) \end{aligned}\right\} \tag{2.51}$$

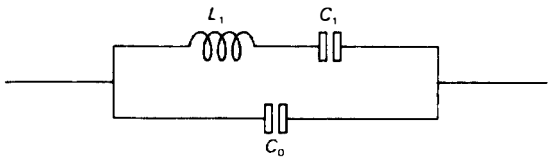

Fig. 2.2 Lossless equivalent circuit.

where c, e and ϵ are the effective elastic, piezoelectric and dielectric constants for the particular excited mode, and are obtained from the defining relations Eqns (2.12), (2.13) and (2.16) when these are expressed in the coordinate system that diagonalizes Γ_{km}.

Although the expressions above are derived only for the special case of pure thickness vibrations, and so cannot be expected to yield accurate numerical results, they nevertheless demonstrate important functional dependencies of the equivalent circuit parameters that are borne out in practice. In particular, the reduction in C_1 and in the capacitance ratio C_1/C_0 with the square of the overtone order means that the 'pulling sensitivity' (Chapter 6) of overtone units is at least an order of magnitude less than that for fundamentals.

In all the analysis of this chapter it has been assumed that the material is non-dissipative, and consequently the derived equivalent circuit contains no resistive element. This assumption can be removed by assuming that the stresses depend not only on the strain but also on the time rate of change of the strain. Ignoring the piezoelectricity for the moment, this means that the stress–strain relationships have to be generalized to

$$T = cS + \eta\dot{S}$$

where the tensor indices have been dropped for simplicity, but nevertheless the *viscosity* η is a fourth rank tensor having the same symmetry properties as the elastic constants c. In a situation where the time dependence is of the form $\exp(j\omega t)$, $\dot{S}$ is just $j\omega S$, and thus the stress–strain relationship is

$$T = (c + j\omega\eta)S$$

In this case then the viscous losses can be taken into account by treating the elastic constants as complex rather than real quantities. The analysis of Section 2.1 can be carried forward with complex elastic constants just as before, up to and including the derivation of the wave equation (Eqn 2.15). The tensor Γ_{km} will now have complex components through the definitions in Eqns (2.11) and (2.16) and will therefore have complex eigenvalues c_m. However, provided the losses are very small, the complex eigenvalue problem can be avoided by ignoring the imaginary part of Γ_{km} and diagonalizing the real part. The imaginary part of the eigenvalue c_m, that is, the effective viscosity in the mth mode, can then be restored by using the analogue of Eqn (2.11), so that

$$\delta_{km}\eta_m = \eta_{klmn}n_l n_m \tag{2.52}$$

with all quantities expressed in the coordinate system in which Γ_{km} is diagonal.

In the wave equation (2.19), c_k is then to be replaced by the complex $c_k + j\omega\eta_k$. The assumed solutions given in Eqn (2.32) must then be augmented by an additional factor $\exp(-\alpha t)$, where α is given by

$$\alpha = (\eta_k \omega^2)/(2c_k) \tag{2.53}$$

Comparing α as given by Eqn (2.53) to the corresponding expression for the damping factor in a series RLC circuit with a quality factor Q leads to the identification

$$R/2L = \omega/(2Q) = (\eta_k \omega^2)/(2c_k)$$

and thus to the following expression for the intrinsic Q of the kth mode

$$Q_k = c_k/(\omega \eta_k) \tag{2.54}$$

In terms of the *time constant* τ_k introduced by Guttwein, Lukaszek and Ballato (Guttwein *et al.*, 1967) and defined by $\tau_k = \eta_k/c_k$

$$Q_k = 1/\omega\tau_k \tag{2.55}$$

If a resistance R_1 is included in the series arm of the equivalent circuit of Fig. 2.2, then the Q of the series arm becomes $Q = \omega L_1/R_1$ or $Q = 1/(\omega R_1 C_1)$. Hence $\tau_k = R_1 C_1$ and so from Eqn (2.51)

$$R_1 = M^2 \pi^2 \eta_k h/(4e^2 A) \tag{2.56}$$

The equivalent circuit including R_1 is shown in Fig. 2.3. The expression (Eqn 2.56) for R_1 only includes the effect of the acoustic attenuation due to the viscosity η of the standing wave system in the resonator. In an actual resonator there will be additional contributions to R_1 due to such factors as mounting losses, atmospheric damping, losses in the electrodes and losses due to imperfect surface finish on the major surface of the resonator. Hence the preceding expression for R_1 should be regarded as giving a lower bound for the R_1 of practical resonators, albeit one which can be approached quite closely by proper resonator design and careful processing.

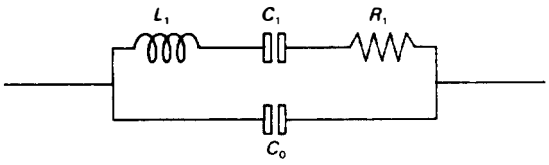

Fig. 2.3 Equivalent circuit of crystal resonator.

2.5 TEMPERATURE COEFFICIENTS OF FREQUENCY

Equation (2.42) determines the anti-resonance frequencies of thickness modes in an infinite plate in terms of the effective elastic constant c_m for the mth mode, the density ρ, and the plate thickness $t = 2h$. The elastic constant

c_m is in turn determined in terms of the fundamental elastic, piezoelectric and dielectric constants through the solution of the eigenvalue problem for the symmetric tensor $\bar{L}_{km}$ defined in Eqn (2.16).

Since all of the material constants and the plate thickness vary with temperature, so too will the anti-resonance frequencies. For a given reference temperature T_0, the rth order temperature coefficient of a function f of the temperature T is defined by

$$T_f^{(r)} = f^{(r)}(T_0)/(r!\, f(T_0)) \tag{2.57}$$

where $f^{(r)}(T_0)$ denotes the rth derivative of $f(T)$ with respect to T evaluated at T_0. By repeatedly differentiating Eqn (2.42) with respect to T, the temperature coefficients of the frequency can be expressed in terms of the coefficients of the effective elastic constant, the density and the plate thickness. In particular, the first-order coefficient of frequency can be immediately obtained as

$$T_f^{(1)} = T_{c_m}^{(1)}/2 - T_\rho^{(1)}/2 - T_t^{(1)} \tag{2.58}$$

$T_\rho^{(1)}$ is independent of the orientation of the plate and is completely determined by the thermal expansion properties of the material. $T_t^{(1)}$ is the effective coefficient of linear expansion in the direction of the plate normal n_k, and thus depends on the thermal expansion coefficients and the orientation. In the notation of Chapter 1, if S_{km} is the thermally induced strain at a temperature T referred to the reference state at temperature T_0, and if $\alpha_{km}^{(r)}$ are the expansion coefficients of order r, then

$$S_{km}(T) = \alpha_{km}^{(1)}(T - T_0) + \alpha_{km}^{(2)}(T - T_0)^2 + \alpha_{km}^{(3)}(T - T_0)^3$$

or to first order

$$S_{km}(T) = \alpha_{km}^{(1)}(T - T_0)$$

From the definition (Appendix 3) of the strain tensor, the fractional change in volume of an elementary volume element accompanying a strain S_{km} is just $S_{kk} = S_{11} + S_{22} + S_{33}$, so that since mass is conserved, the corresponding fractional change in the density is just $-S_{kk}$. Hence the first-order temperature coefficient of the density is just

$$T_\rho^{(1)} = -\alpha_{kk}^{(1)} = -(\alpha_{11}^{(1)} + \alpha_{22}^{(1)} + \alpha_{33}^{(1)}) \tag{2.59}$$

Also, again from the definition of S_{km}, the fractional change in length of a line element along the direction n_k is $S_{km}n_kn_m$, so that the effective coefficient of linear expansion along n_k is

$$T_t^{(1)} = \alpha_{km}^{(1)}n_kn_m \tag{2.60}$$

From the data given in Table 1.1, it follows that $T_\rho^{(1)}$ has the value -34.9 ppm/°C. The maximum value for $T_t^{(1)}$ occurs when n_k is perpendicular to the optic axis and is $\alpha_{11}^{(1)}$ or 13.71 ppm/°C, while the minimum occurs when n_k is along the optic axis and is $\alpha_{33}^{(1)}$ or 7.48 ppm/°C. Hence the contribution

of the last two terms in Eqn (2.58) to the first-order temperature coefficient of frequency varies from a minimum of +3.74 ppm/°C with n_k perpendicular to the optic axis, to a maximum of +9.97 ppm/°C for n_k along the optic axis. Since the values of the first-order coefficients of the fundamental elastic constants, which are the major determinants of the effective elastic constant c_m, are typically an order of magnitude greater than these contributions, it follows that the temperature coefficient of frequency is primarily determined by the temperature coefficients of the elastic constants.

So far, the discussion has been limited to the anti-resonance frequencies, although in practice it is usually the resonance frequencies that are of more interest. As has already been pointed out in Section 2.3, in the general case where all three thickness modes are excited, the resonance frequencies have to be determined as solutions of Eqn (2.43). Fortunately, for the important quartz cuts it is usually sufficient to consider the case where either only one mode is excited, or where, even if two or more modes are present, their resonance frequencies are sufficiently far separated for the single-mode analysis to be used.

The key result in the single-mode case is Eqn (2.48), which relates the fractional frequency difference between the anti-resonance and resonance frequencies to the electromechanical coupling factor for the mode under consideration. Writing f_A and f_R for the anti-resonance and resonance frequencies and dropping the suffix m identifying the particular mode, Eqn (2.48) can be rewritten

$$(f_A - f_R)/f_A = 4k^2/M^2\pi^2$$

or

$$f_R = f_A\,(1 - 4k^2/M^2\pi^2) \tag{2.61}$$

Differentiating Eqn (2.61) and making use of the fact that in quartz the coupling factor k^2 is always $\ll 1$ leads then to the result

$$T_{f_R}^{(1)} = T_{f_A}^{(1)} - 8k^2\,T_k^{(1)}/M^2\pi^2 \tag{2.62}$$

with $T_k^{(1)}$ being the first-order temperature coefficient of the coupling factor. It follows immediately from Eqn (2.62) that the difference between the temperature coefficients of the resonance and anti-resonance frequencies decreases rapidly with both increasing overtone order and decreasing coupling.

Analytical expressions for the higher order temperature coefficients of frequency in terms of the higher order coefficients of the material constants can be developed by further differentiation of the basic frequency equation (2.42). However, these expressions rapidly become cumbersome as the order increases, and it is usually easier to determine higher order coefficients by numerical methods.

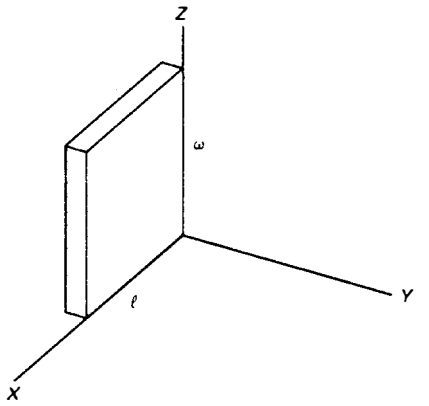

Fig. 2.4 (*YX*) crystal plate.

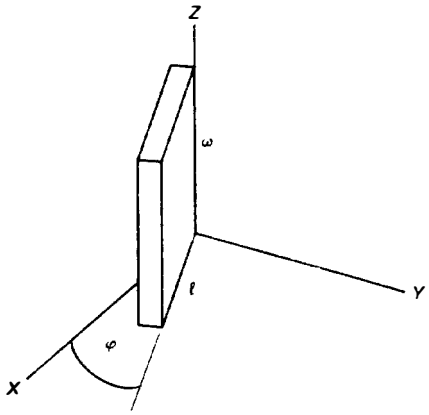

Fig. 2.5 (*YXw*) ϕ crystal plate.

2.6 DOUBLY ROTATED CUTS

The 1978 *IEEE Standard on Piezoelectricity* (IEEE, 1978) describes a general method of specifying a crystal plate that is arbitrarily oriented with respect to the crystallographic axes *OXYZ*. The application of this method to generally oriented thickness mode resonators is as follows. Choose as a starting point a *Y*-cut plate of length *l*, width *w* and thickness *t*, with the length along *OX*, width along *OZ* and thickness along *OY* (Fig. 2.4). This plate has the simple notation (*YX*), where the first symbol indicates the axis along which the thickness lies and the second the axis along which the length *l* lies. The (*YX*) plate is then rotated about its width, that is about *OZ*, through an angle ϕ (Fig. 2.5). This singly rotated plate then has the notation (*YXw*)ϕ

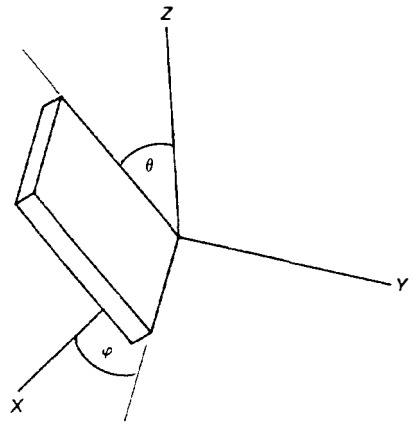

Fig. 2.6 (*YXwl*) ϕ/θ crystal plate.

where w indicates the axis of the rotation and ϕ its magnitude. A second rotation of magnitude θ is then applied about the length of the (*YXw*) plate, to produce a *doubly rotated* plate described by the notation (*YXwl*) ϕ/θ (Fig. 2.6).

The IEEE standard goes on to describe triply rotated plates, but for pure thickness modes the doubly rotated plate covers all possibilities as the third rotation would be about the plate normal and would therefore not alter the physical situation. (This of course assumes a plate of effectively infinite lateral extent.) In the case of quartz, having trigonal symmery about the optic axis OZ and digonal symmetry about OX, it is easily seen that for a doubly rotated plate, the angle range $\phi = 0°$ to $\phi = 30°$ covers all eventualities, with θ ranging over $-90°$ to $+90°$. The plate normal n_k initially lies along OY and so has components (0,1,0). The components n_k of the normal to the doubly rotated plate are obtained by applying the rotation matrices (Appendix 5) for the ϕ and θ rotations to the initial vector (0,1,0), and are

$$\begin{aligned} n_1 &= -\cos(\theta)\sin(\phi) \\ n_2 &= +\cos(\theta)\cos(\phi) \\ n_3 &= \sin(\theta) \end{aligned} \tag{2.63}$$

The analysis of thickness modes in the preceding sections, together with a set of values for the fundamental material constants and their temperature coefficients, in principle allows the theoretical prediction of the key properties of a thickness mode resonator as functions of the orientation angles ϕ and θ. In particular, the frequency–thickness constants and the electromechanical coupling factors for each mode can be calculated as a function of temperature and orientation. By curve-fitting the data so obtained, the first and higher order temperature coefficients of the anti-

Table 2.1 Doubly rotated crystal cuts

Cut	AT	FC	IT	SC	LC	BT	RT
ϕ	0	15	19.10	21.93	11.17	0	15
θ	−35.25	−34.33	−34.08	−33.93	− 9.39	49.20	34.50
k_a	0	2.37	2.96	3.33	3.21	0	4.27
k_b	0	3.61	4.33	4.71	7.64	5.62	6.46
k_c	8.8	6.89	5.79	4.99	9.21	0	2.12
N_a	3504	3446	3411	3382	3165	3089	3059
N_b	1900	1936	1959	1977	2140	2536	2260
N_c	1661	1726	1766	1797	1727	1884	2040
$T_a^{(1)}$	−48.9	−50.1	−51.2	−52.1	−26.1	−95.6	−74.6
$T_b^{(1)}$	−31.3	−29.1	−27.5	−26.2	−39.7	0	− 1.49
$T_c^{(1)}$	0	0	0	0	39.8	−30.9	0

Note: 1 Coupling factors k_a, k_b and k_c in %.
2 Frequency constants N_a, N_b and N_c in kHz mm.
3 Temperature coefficients $T_a^{(1)}$, $T_b^{(1)}$ and $T_c^{(1)}$ in ppm/°C.

For further detail, refer to Ballato (1977).

resonance frequencies, the coupling, and the resonance frequencies can easily be obtained.

Table 2.1 lists some of these principal characteristics of the better known doubly rotated cuts. The Table gives the commonly used designation for each cut, the approximate ϕ and θ angles, and the coupling factors, frequency constants, and first-order frequency–temperature coefficients for the three possible thickness modes in each orientation. The modes are identified in accordance with the usual conventions (Ballato, 1977) as *a*, *b* and *c* modes, with the phase velocities being ordered as $V_a > V_b > V_c$. Although the classification of the modes as longitudinal and transverse is not generally valid (cf. Section 2.1), nevertheless the *a* mode is commonly referred to as the *quasi-longitudinal* mode, and the *b* and *c* modes as the *fast shear* and *slow shear* mode, respectively. (It should be noted that in Table 2.1 and elsewhere in this book, the 1978 *IEEE Standard on Piezoelectricity* has been followed in adopting sign conventions for the crystallographic axes. This means that the sign of the θ angle is reversed compared to the conventions adopted in much of the earlier work.)

The special cases of the AT- and BT-cuts, which have $\phi = 0°$ and belong to the rotated *Y*-cut family, are considered in more detail in the following sections, but are included here for purposes of comparison. All of the cuts listed with the exception of the LC-cut have a zero first-order temperature coefficient of frequency for either the *b* mode or the *c* mode at around room temperature. The LC-cut is included because the second and third order coefficients for the *c* mode vanish, resulting in an ultra-linear frequency–temperature characteristic useful in precision thermometry.

The IT cut (Bottom and Ives, 1951), RT-cut (Bechmann, 1961) and the FC-cut (Lagasse *et al.*, 1972) are all cuts introduced for the main purposes of

improving upon the well established AT-cut's performance in certain applications. The typical AT frequency–temperature characteristic (Section 2.8) is cubic in character, with a negative slope at room temperature and turning points symmetrically located about a point of inflexion at or just above room temperature. In applications where the frequency stability requirements are such as to make temperature control of the crystal necessary, it is standard practice to place the crystal in an oven whose operating temperature is set to the upper turnover point of the crystal, so that the frequency–temperature coefficient is zero at the oven temperature. For the AT this requires that oven temperature and crystal turnover be closely matched in order to obtain acceptable results.

The principal difference between the AT- and the FC-cut is that in the latter the inflexion temperature is much higher. This means that for a given oven temperature T, an FC-cut with an upper turning point T will have a relatively much flatter frequency–temperature curve than a corresponding AT. This can be taken advantage of in one of two ways: either to obtain improved stability from a given oven, or to relax the oven requirements in respect of temperature stability while maintaining the frequency stability. A subsidiary advantage of the higher inflexion point is that the frequency deviation from room temperature to oven temperature is much less than with the AT. These points are illustrated in Fig. 2.7.

Although of considerable significance, these advantages have not been the major factor in the increased use of doubly rotated cuts. The predictions in 1974 and 1975 of plate orientations minimizing certain non-linear effects, along with their later experimental confirmation, provided the impetus for the continuing use of doubly rotated resonators. Holland (1974a, b) first predicted that at an orientation of $\phi = 22.8°$, $\theta = -34.3°$ thermal shocks would produce no frequency excursions or transients, and coined the term

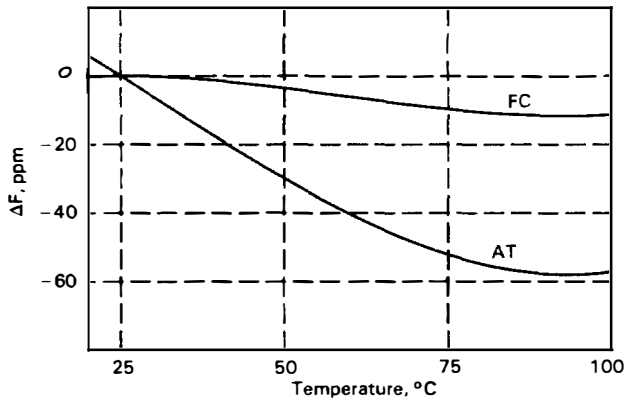

Fig. 2.7 Comparison of AT and FC characteristics.

TS-cut (for *t*hermal *s*hock). In the following year, EerNisse (1975) similarly predicted that at an orientation of $\phi = 22.5°$, $\theta = -34.3°$, frequency changes due to mechanical stresses in the plane of the resonator plate would be minimized and introduced the term *SC-cut* for *s*tress *c*ompensated). It is now generally recognized that these cuts are essentially the same, and the SC-cut nomenclature is commonly accepted. The main advantages and disadvantages of the SC-cut versus the AT-cut have already been summarized in Section 1.4.7.

2.7 ROTATED *Y*-CUTS

In an arbitrarily oriented crystal plate, the effective symmetry of the device is much reduced as compared to the symmetry of the material. In general both the electric and the optic axes, which are, respectively, digonal and trigonal symmetry axes, will make oblique angles with the edges of the plate. However, in those special cases where the plate axes include one of the crystal symmetry axes, it is to be expected that the performance of the resonator will reflect this symmetry in some respects. This is true in particular of the rotated *Y*-cut family of plates $(YXwl)\phi/\theta$ with $\phi = 0°$. Since $\phi = 0$, an equivalent notation is simply $(YXl)\,\theta$.

In such plates, the length l is originally along the X or electric axis, and this is the axis about which the plate is rotated. Thus the X axis is contained in the plane of the plate for all members of the rotated Y-cut family, and consequently the plate normal n_k has no component along X, $n_1 = 0$. From Eqn (2.63), the components of n_k are just $(0, \cos(\theta), \sin(\theta))$.

Setting $n_1 = 0$ and using the symmetry relations that exist among the fundamental material constants of quartz (Section 1.3), the effective dielectric and piezoelectric constants ϵ and e_k defined in Eqns (2.13) and (2.12) reduce to the simple forms

$$\epsilon = \epsilon_{km} n_k n_m = \epsilon_{11} n_2^2 + \epsilon_{33} n_3^2 \tag{2.64}$$

$$\begin{aligned} e_1 &= -e_{11} n_2^2 - e_{14} n_2 n_3 \\ e_2 &= e_3 = 0 \end{aligned} \tag{2.65}$$

Similarly, from the defining equation for L_{km}, Eqn (2.11),

$$\begin{aligned} L_{11} &= c_{66} n_2^2 + c_{44} n_3^2 + 2c_{14} n_2 n_3 \\ L_{12} &= L_{13} = 0 \end{aligned} \tag{2.66}$$

Using Eqns (2.65) and (2.66) with the definition Eqn (2.16) of Γ_{km} gives finally

$$\begin{aligned} \Gamma_{11} &= L_{11} + e_1^2/\epsilon \\ \Gamma_{12} &= \Gamma_{13} = 0 \end{aligned} \tag{2.67}$$

Equations (2.65) and (2.67), in conjunction with the wave equation (2.15), the expression for the electrostatic potential (2.14), and the expressions for the surface tractions and electric displacement in Eqns (2.17) and (2.18), show that the mechanical displacement u_1 is not coupled to the displacements u_2 and u_3, and is the only displacement coupled to the electric field. This leads directly to the key result that for the rotated Y-cuts, the only one of the three possible thickness modes that can be piezoelectrically excited must be a pure thickness shear with the displacement along the X axis. The relevant wave equation is

$$\bar{L}_{11}u_{1,xx} = \rho\ddot{u}_1 \tag{2.68}$$

The accompanying electric potential is

$$\phi = e_1u_1/\epsilon + Cx + D \tag{2.69}$$

and the electromechanical coupling factor is

$$k^2 = e_1^2/\epsilon\bar{L}_{11} \tag{2.70}$$

From Eqn (2.42), the frequency–thickness constant N follows as

$$N = 2hf = (\bar{L}_{11}/\rho)^{1/2}/2 \tag{2.71}$$

Figures 2.8 and 2.9 show the variation of the coupling factor and the frequency–thickness constant with the rotation angle θ. Because the term e_1^2/ϵ in Eqn (2.67) represents only a small correction to L_{11}, to a good approximation the extreme values of N coincide with those of L_{11}. Differentiation of Eqn (2.66) shows that these extrema occur at angles such that

$$\tan(2\theta) = 2c_{14}/(c_{66} - c_{44}) \tag{2.72}$$

Reference to Appendix 5 shows that this also gives the angles at which the elastic constant c_{56}', expressed in the plate coordinate system, vanishes. As

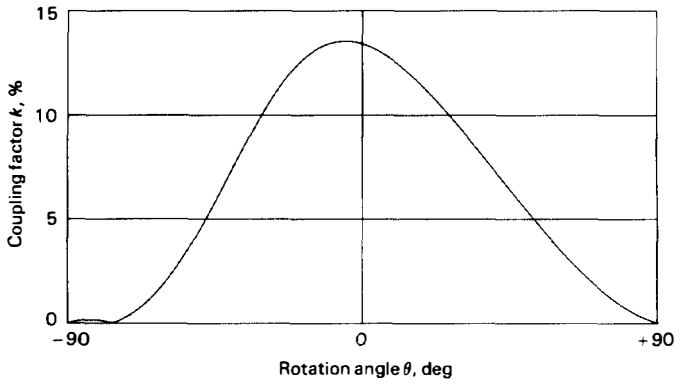

Fig. 2.8 Coupling factor for rotated Y-cut plates.

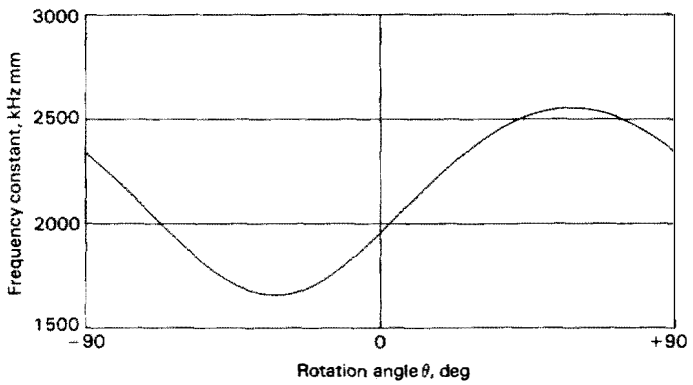

Fig. 2.9 Frequency constant for rotated Y-cut plates.

already stated in Section 1.4.7, the solutions of Eqn (2.72) are $-31.6°$ and $+58.4°$, corresponding, respectively, to the AC- and BC-cuts.

The first-order temperature coefficient of the anti-resonance frequency is determined by Eqn (2.58), with the dominant term being $T^{(1)}_{c_m}$. In the present case, the effective elastic constant is Γ_{11}, or to a good approximation, L_{11}. Differentiating Eqn (2.66) with respect to the temperature leads to the following expression for the first-order coefficient of L_{11} in terms of the coefficients of the fundamental elastic constants

$$T^{(1)}_{L_{11}} = (c_{66}T^{(1)}_{c_{66}}n_2^2 + c_{44}T^{(1)}_{c_{44}}n_3^2 + 2c_{14}T^{(1)}_{c_{14}}n_2n_3)/L_{11} \tag{2.73}$$

Fig. 2.10 shows $T^{(1)}_{L_{11}}$ as a function of orientation. There are two angles θ where small negative values of $T^{(1)}_{L_{11}}$ compensate for the net positive contribution of $T^{(1)}_{\rho}$ and $T^{(1)}_{t}$ to give a zero temperature coefficient of frequency. These angles correspond to the AT- and BT-cuts, at $\theta = -35.25°$ and $\theta = +49.2°$, respectively.

2.8 AT-CUT RESONATORS

Table 2.2 lists the values of the key physical parameters for the AT-cut resonator as determined from the expressions derived in the previous section. The term AT-cut is in practice applied to resonators that have a range of θ values of the order of $1°$ around the nominal AT angle, and there will be slight variations in the values of the parameters in Table 2.2 depending on the precise angle used. However, the errors resulting from the thickness mode approximation generally make it unnecessary to take account of errors due to slight angle differences.

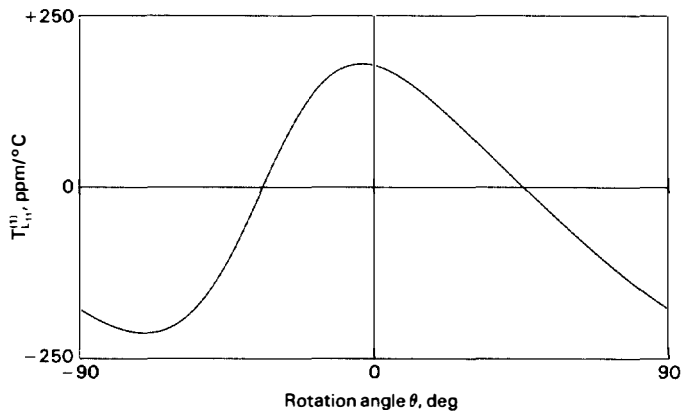

Fig. 2.10 $T_{L_{11}}^{(1)}$ for rotated Y-cut plates.

Table 2.2 Physical parameters for AT-cut resonators

ϕ angle	0°
θ angle	−35.25°
Density	2649 kg/m^3
Effective elastic constant	29 × 10^9 N/m^2
Effective piezoelectric constant	0.095 C/m^2
Effective dielectric constant	40.3 × 10^{-12} F/m
Frequency constant	1660 kHz/mm
Coupling factor	8.74%

The defining feature of both AT- and BT-cuts is the vanishing of their first-order temperature coefficients at room temperature. In principle, the higher order coefficients could be calculated from the corresponding coefficients of the fundamental material constants, but in practice it turns out that the frequency–temperature characteristics of both AT- and BT-cuts are known empirically with more precision than can be obtained by calculation. Thus the situation is often reversed, in that the material properties are inferred from the frequency–temperature characteristics rather than vice versa.

Bechmann (1955, 1956, 1960) has established that for both AT- and BT-resonators, their frequency–temperature characteristics over a wide temperature range can be adequately described by a power series in the temperature including terms up to third order. Writing f for the frequency at a temperature T, and f_0 for the frequency at a reference temperature T_0, Bechmann's expression is

$$(f - f_0)/f_0 = a(T - T_0) + b(T - T_0)^2 + c(T - T_0)^3 \tag{2.74}$$

Bechmann also found that within small angle ranges about the nominal

angles for the AT and BT, the coefficients a, b and c could be expressed as linear functions of the angle increment $\Delta\theta$ from some predefined reference angle. Thus a can be written

$$a = a_0 + a_1\Delta\theta \tag{2.75}$$

with similar expressions for b and c.

Although Eqn (2.74) applies to both AT and BT resonators, the relative magnitude of the various terms is quite different. In the AT the cubic term is the dominant one, giving rise to the typical 'S' shaped characteristics shown in Fig. 2.11, whereas the quadratic term is dominant in the BT. Hence the BT characteristics are parabolic in nature, as shown in Fig. 2.12, making the BT much less suitable for applications involving wide temperature ranges.

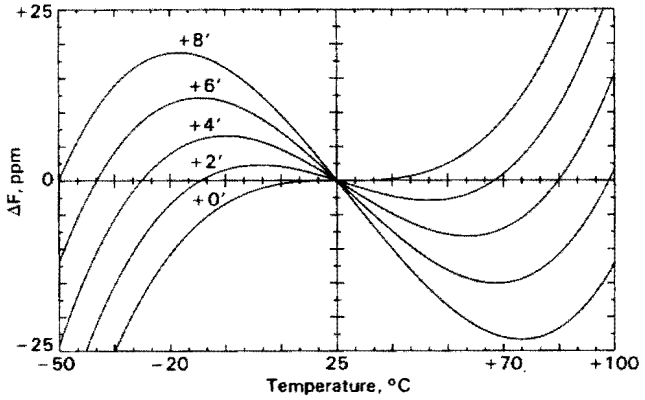

Fig. 2.11 Normalized AT-cut curves.

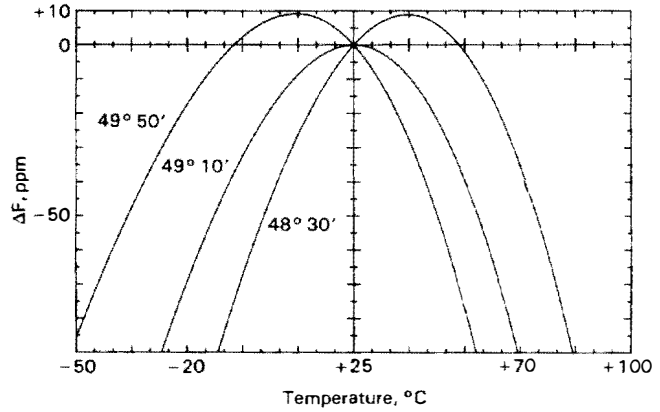

Fig. 2.12 Normalized BT-cut curves.

Table 2.3 Bechmann's coefficients for the AT-cut resonator

Reference temperature	20°C
Reference angle	−35°15′
Coefficients	
a_0	0
a_1	$-5.15 \times 10^{-6}/°C/°\theta$
b_0	$0.39 \times 10^{-9}/(°C)^2$
b_1	$-4.7 \times 10^{-9}/(°C)^2/°\theta$
c_0	$109.5 \times 10^{-12}/(°C)^3$
c_1	$-2.0 \times 10^{-12}/(°C)^3/°\theta$

Table 2.3 gives Bechmann's 1960 values of a_0, a_1, etc, for the AT resonator, referred to $T_0 = 20°C$ and a reference angle of $-35.25°$. It should be borne in mind in using this data that the values were arrived at by analysis of results from a wide range of resonators of different detailed design, and should be applied with caution in particular cases. In particular, the choice of reference angle required to fit the measured data in a specific case is a sensitive function of the resonator design, depending strongly on the overtone, the geometry of the blank, and the electrical operating conditions. These are considered in more detail in Chapter 7.

Nonetheless, the main features of the frequency–temperature characteristics of AT cut resonators can be seen using the data of Table 2.3. Fig. 2.11 shows the typical characteristics for a range of angle increments $\Delta\theta$. As the angle increases, the slope of the curves at room temperature becomes increasingly negative, while at the same time the separation between the turning points and the accompanying frequency deviation increases. The large scope for trading frequency stability against operating temperature range is apparent from the Figure, and has been the main factor in making the AT resonator the most commonly used crystal unit in a wide range of applications.